Hindawi
Geofluids
Volume 2020, Article ID 6671479, 8 pages
https://doi.org/10.1155/2020/6671479

Research Article

Effect of Porosity on Soil-Water Retention Curves: Theoretical and Experimental Aspects

Chang Liu,[1,2] Fuguo Tong,[2] Long Yan,[3] Hongbo Zhou,[4] and Shuang Hao[5]

[1]*College of Hydraulic & Environmental Engineering, China Three Gorges University, Yichang 443002, China*
[2]*Key Laboratory of Geological Hazards on Three Gorges Reservoir Area (China Three Gorges University), Ministry of Education, Yichang 443002, China*
[3]*Institute of Geotechnical Engineering, Hohai University, Nanjing 210098, China*
[4]*Nonferrous Geological Exploration and Research Institute Limited Liability Company, Shenyang 110013, China*
[5]*Department of Sustainable Development, Environmental Science and Engineering, KTH Royal Institute of Technology, S-10044 Stockholm, Sweden*

Correspondence should be addressed to Fuguo Tong; tfg_ctgu_edu@163.com

Received 12 November 2020; Revised 25 November 2020; Accepted 2 December 2020; Published 22 December 2020

Academic Editor: Feng Xiong

Porosity change is a common characteristic of natural soils in fluid-solid interaction problems, which can lead to an obvious change of the soil-water retention curve (SWRC). The influence of porosity on soil water retention phenomena is investigated by a theoretical model and an experimental test in this study. A model expressing the change in suction with porosity and effective saturation is put forward theoretically. The model is based on an idealization of three-phase porous materials, the pore structures of which are homogeneous and isotropic. It accounts for the porosity effect on soil water retention, using four parameters with clear physical meanings. The presented model can obtain the SWRC at any porosity, which will reduce the test number required in characterizing the hydraulic behavior of soil. A laboratory experiment for loamy sand with different porosities is performed. The test results show that suction has a significant variation with changes in porosity and decreases with the increase of porosity. The formulation is verified by both the test data and the literature data for FEBEX bentonite and Boom clay. The very good agreements between measured and predicted results show that the SWRC model is reliable and feasible for various soils.

1. Introduction

The soil-water retention curve (SWRC) is defined as the relationship between matric suction and the degree of saturation in unsaturated soils. The SWRC relation is a key hydraulic property to describe fluid flow phenomena in unsaturated soils, which can be affected by the porosity or the density of the soil [1, 2]. A variation in soil porosity is common in fluid-solid interaction problems [3, 4], and this change will result in an obvious change of SWRC [5]. Sometimes, it needs to predict the SWRCs for soil with different porosities. However, many traditional SWRC models [6–11] do not consider the effect of porosity on SWRC, which may cause an inaccurate result. Therefore, it needs to establish the relationship between porosity and SWRC in agricultural engineering and geotechnical engineering, especially involving water-induced landslides [12–14] and water-rock coupling engineering [15–17].

Various SWRC models have been proposed to take the influence of porosity into account by relating suction and/or the pore size distribution index to void ratio or density. The first group of the models linked the current void ratio to the initial void ratio using a volume change law which describes the relation between suction and void ratio [18–22]. It is difficult to establish a direct formulation between volume and suction, which usually involves the hydraulic and mechanical processes of soil. Some models used an empirical volume function to quantify the influence of initial porosity on SWRC based on experimental findings [21]. Even for the simplest models [23], it still requires a lot of additional parameters to describe the

variation of soil volume. The other approaches describe the porosity dependence by shifting SWRCs with a porosity-dependent air entry value or pore size distribution index [3, 24–28]. Such approaches can be used in SWRC laws which contain the item of air entry value, such as the Brooks and Corey model [7]. But unsaturated soils are three-phase mixtures of solid, water, and air. Water and air flow in structured soils depend not only on soil texture but also on pore shape and pore distribution [29]. Some important intrinsic relations for the pore systems may not be satisfied. It is necessary to consider the influence of pore distribution, shape, and size on SWRC from the mixture theory.

In this paper, a SWRC model accounting for the effect of porosity is presented, assuming the unsaturated soil as a continuous, isotropic, and homogeneous three-phase pore mixture. This equation is expressed by a law of effective saturation, suction, and porosity, with only four parameters. An experimental test is also conducted for loamy sand to study the porosity effect on water retention. The proposed model is verified by the test data for loamy sand with different porosities, as well as the literature data for FEBEX bentonite and Boom clay.

2. Derivation of the Porosity-Dependent SWRC Model

Suction, s, can be expressed as the relation between pore gas pressure (u_g) and pore water pressure (u_w):

$$s \equiv u_g - u_w. \tag{1}$$

u_g in soil can be set as the atmospheric pressure, for gas flow is relatively free to the water flow ([30, 31]). Therefore, it only needs to determine u_w.

2.1. Pore Water Pressure. Although the soil pore structure is composed of nonuniform pore size and the pore distribution is quite complex, most soils can be assumed to be a continuous, isotropic, and homogeneous porous medium, in which the distributions of pore water and air are also isotropic and homogeneous at a macroscopic scale [29]. Therefore, on per unit area of two-dimensional (2D) cross-section cutting through the soil for any angle, the total pore area A_p, pore gas area A_g, and pore water area A_w are constant. The macroscopic porosity ϕ and saturation S_r can be described by

$$\begin{aligned} \phi &= \frac{V_p}{V} = \frac{A_p}{A}, \\ S_r &= \frac{V_w}{V_p} = \frac{A_w}{A_p}, \end{aligned} \tag{2}$$

where V_p, V_w, and V are the total volume of pore, water, and soil, respectively.

The water in the pore mainly includes the interfaces of water-solid and water-gas and the water between the two interfaces, as shown in Figure 1(a). In order to calculate u_w on any cross-section, the pore shape can be arbitrary. Here, the pores are idealized as ellipses for their shape can be round or flat. An elliptical pore randomly distributes on arbitrary cross-section. Each pore contains an identical elliptic air bubble (Figure 1(b)) [29]. The total normal force of a given cross-section is expressed as

$$F_w = -\int_{T_{w\text{-}g}} T_s \sin\alpha \mathrm{dl} + \iint_{D_w} u_w' dA, \tag{3}$$

where T_s represents water surface tension, α is the angle between the tangent plane and the section plane at point C of the water-gas interface (Figure 1(b)), and dl represents the differential length of $T_{w\text{-}g}$. D_w is the area occupied by water but not including the water-gas interface. The differential area of D_w is represented by $dA\mu_w'$ represents the static water pressure in the area of D_w.

According to the assumption of isotropy and homogeneity of medium, the angle at any point at the water-air interface always has $0 \le \alpha \le \pi$. The part, $-T_s\int_{T_{w\text{-}g}} \sin\alpha \mathrm{dl}$, in Eq. (3) can be expressed as

$$-T_s\int_{T_{w\text{-}g}} \sin\alpha \mathrm{dl} = -T_s\int_L \sin\frac{\pi l}{L}\mathrm{dl} = -T_s\frac{2L}{\pi}. \tag{4}$$

Another part, $\iint_{D_w} u_w' dA$, in Eq. (3) is rewritten as

$$\iint_{D_w} u_w' dA = \overline{u'}_w A_w. \tag{5}$$

According to the theory of surface science, the surface tension of liquid can be regarded as a constant when temperature is constant [32]. u_w can be described as

$$u_w = \frac{F_w}{A_w} = -k\frac{L}{A_w} + \bar{u}_w', \tag{6}$$

where $k = 2T_s/\pi$; the unit for k is N/m.

The shapes of elliptic gas bubbles and pores are represented by two semiaxes, a_1 and b_1 for pores ($a_1 \ge b_1$) and a_2 and b_2 for gas bubbles ($a_2 \ge b_2$). A pore contains gas bubble, so there are $b_2 \ge b_1 \ge 0$ and $a_2 \ge a_1 \ge 0$. Defining $e_1 = b_1/a_1$ and $e_2 = b_2/a_2$, where $0 < e_1 \le 1$ and $0 < e_2 \le 1$, the macroscopic porosity ϕ and saturation S_r can be expressed as

$$\phi = \frac{V_p}{V} = \frac{A_p}{A} = \frac{n\pi {a_1}^2 e_1}{A}, \tag{7}$$

$$S_r = \frac{V_w}{V_p} = \frac{A_w}{A_p} = \frac{n\pi\left({a_1}^2 e_1 - {a_2}^2 e_2\right)}{n\pi {a_1}^2 e_1} = 1 - \frac{e_2}{e_1}\left(\frac{a_2}{a_1}\right)^2. \tag{8}$$

The equivalent pore number per area for the cross-section is represented by η, which is expressed as $\eta = n/A$. According to Eqs. (7) and (8), one can obtain $a_1 = (\phi/\eta\pi e_1)^{0.5}$ and $a_2 = a_1[e_1/e_2(1 - S_r)]^{0.5}$.

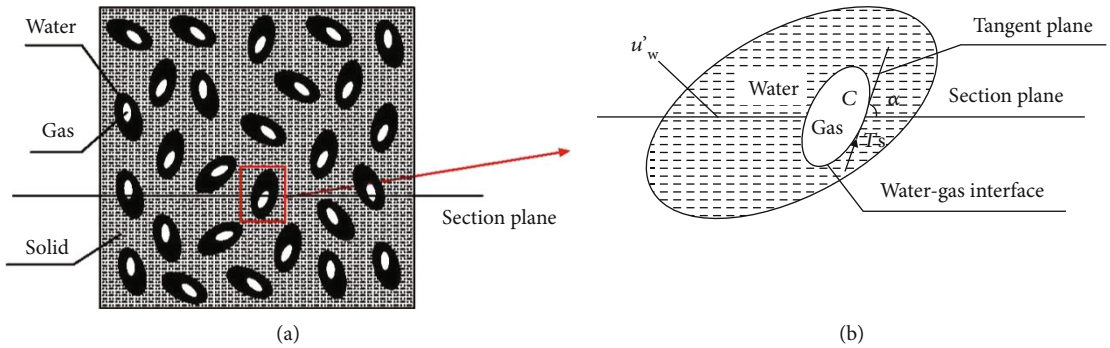

FIGURE 1: (a) Ideal pore structure and the distribution of water, gas, and solid; (b) angle α at point C.

The perimeter of an elliptical air bubble can be written as $L_1 = 2\pi\sqrt{(a_2^2 + b_2^2)/2} = \pi a_2\sqrt{2(1+e_2^2)}$. The total perimeter length of the air bubbles on the cross-section:

$$L = nL_1 = n\pi a_2\sqrt{2(1+e_2^2)} = n\left(\frac{\phi}{\eta}\right)^{0.5}(1-S_r)^{0.5}\left(2\pi e_2 + 2\pi e_2^{-1}\right)^{0.5},$$
$$A_w = A_p - A_a = n\pi\left(a_1^2 e_1 - a_2^2 e_2\right) = \frac{n\phi S_r}{\eta}. \tag{9}$$

Eq. (6) can be rewritten as

$$u_w = -k\left(\frac{\eta}{\phi}\right)^{0.5}\frac{(1-S_r)^{0.5}}{S_r}\left(2\pi e_2 + 2\pi e_2^{-1}\right)^{0.5} + \bar{u}_w'. \tag{10}$$

2.2. Formulations of the New SWRC Model. Substituting Eq. (10) into Eq. (1) yields

$$s = k\left(\frac{\eta}{\phi}\right)^{0.5}\frac{(1-S_r)^{0.5}}{S_r}\left(2\pi e_2 + 2\pi e_2^{-1}\right)^{0.5} - \bar{u}_w'. \tag{11}$$

The equation of suction is composed of the functions of pore density, saturation, shape of air bubbles, and water stress. The influence of porosity on suction is reflected through the parameters ϕ (porosity), η (pore density), and e_2 (shape coefficient of air bubble). η (pore density) is related to the pore structure of soil and can be written as a function of porosity. A simple function $\eta = c_1\phi^{c_2}$ is used to express the relation. $\bar{u}_w'$ is related to saturation, and its effect can be expressed by saturation. So, Eq. (11) can be rewritten as

$$s = d_1\phi^{d_2}\left(2\pi e_2 + 2\pi e_2^{-1}\right)^{0.5}\frac{(1-(aS_r+b))^{0.5}}{aS_r+b}, \tag{12}$$

where $d_1 = kc_1^{0.5}$, d_1 is in units of N/m^2, and the other parameters are dimensionless. a and b are parameters changed with $\bar{u}_w'$.

Defining $S_e = aS_r + b$ yields

$$s = d_1\phi^{d_2}\frac{(1-S_e)^{0.5}}{S_e}\left(2\pi e_2 + 2\pi e_2^{-1}\right)^{0.5}. \tag{13}$$

S_e can be obtained from the conditions that $S_e(S_r = S_{r\,\max}) = 1$ and $S_e(S_r = S_{r\,\min}) = 0$:

$$\begin{cases} aS_{r\,\max} + b = 1 \\ aS_{r\,\min} + b = 0 \end{cases} \Rightarrow \begin{cases} a = \dfrac{1}{S_{r\,\max} - S_{r\,\min}}, \\ b = \dfrac{-S_{r\,\min}}{S_{r\,\max} - S_{r\,\min}}. \end{cases} \tag{14}$$

Hence, one has

$$S_e = \frac{S_r - S_{r\,\min}}{S_{r\,\max} - S_{r\,\min}}. \tag{15}$$

The equation is not a new one and has been used by many people (including Brooks and Corey and van Genuchten). S_e describes the ratio of current saturation to the maximum. Noting that $S_{r\,\max}$ represents the saturation when $s(S_r = S_{r\,\max}) \equiv s_{\min} = 0$ and $S_{r\,\min}$ represents the saturation when $s(S_r = S_{r\,\min}) \equiv s_{\max}$.

The function $f(e_2) = \left(2\pi e_2 + 2\pi e_2^{-1}\right)^{0.5}$ represents the effect of the shape of air bubbles. It can be approximately expressed by a simple power law function through a good curve fitting method (Figure 2):

$$f(e_2) = 2.5908e_2^{-0.494}. \tag{16}$$

The air bubble shape, represented by e_2, should vary with S_e, ϕ, T (temperature), and some other factors. For the difficulty in measuring e_2 directly in practice or developing analytical function form of e_2, a function for e_2 is used here for simplicity, $e_2 = S_e^{(d_3+d_4\phi)}$, where d_3 and d_4 are parameters related to the concerned soil. Eq. (13) can be simplified as

$$s = d_1\phi^{d_2}\frac{(1-S_e)^{0.5}}{S_e^{(d_3+d_4\phi)}}. \tag{17}$$

The proposed model involves four parameters, $\{d_1, d_2, d_3, d_4\}$. d_1 is related to the surface tension. The unit of d_1 is N/m^2, and the other parameters are dimensionless. d_2 is connected to pore density and related to porosity. d_3 represents the combined effect of temperature, hysteresis effects, and other factors, and d_4 is only related to porosity.

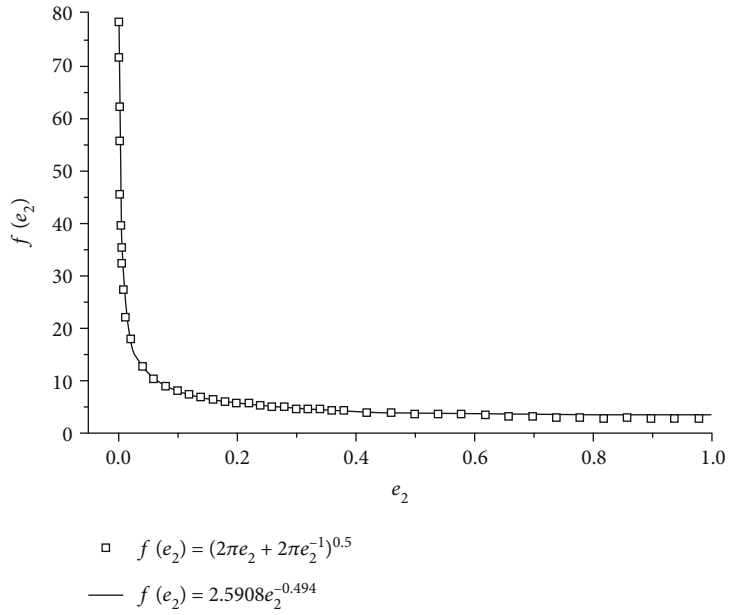

Figure 2: Theoretical and fitting functions of $f(e_2)$.

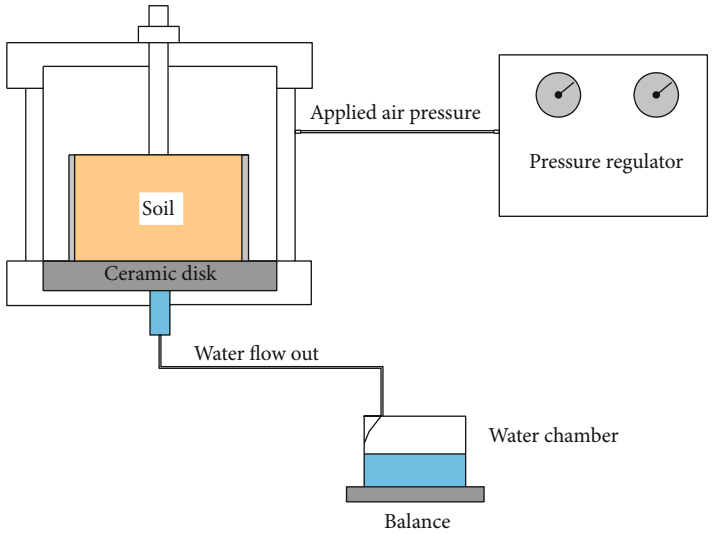

Figure 3: Sketch of test device.

Figure 4: The soil samples.

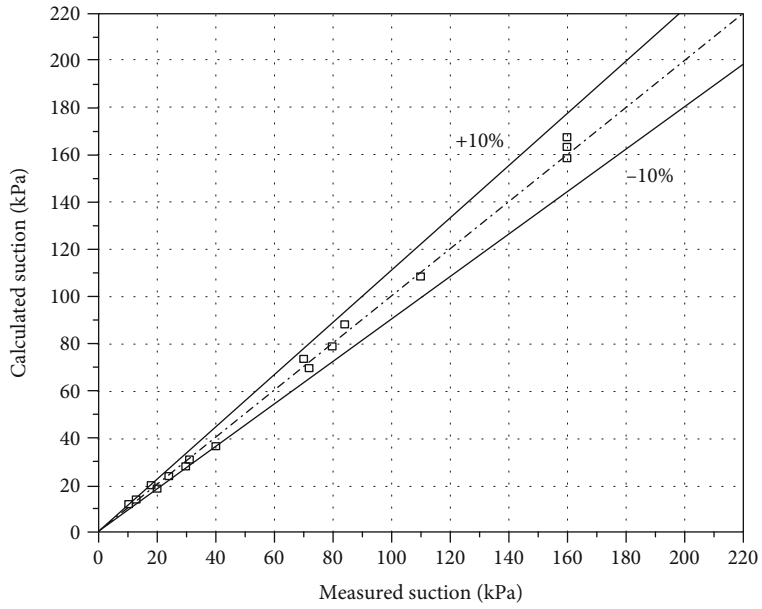

Figure 5: Comparison between experimental and predicted suctions.

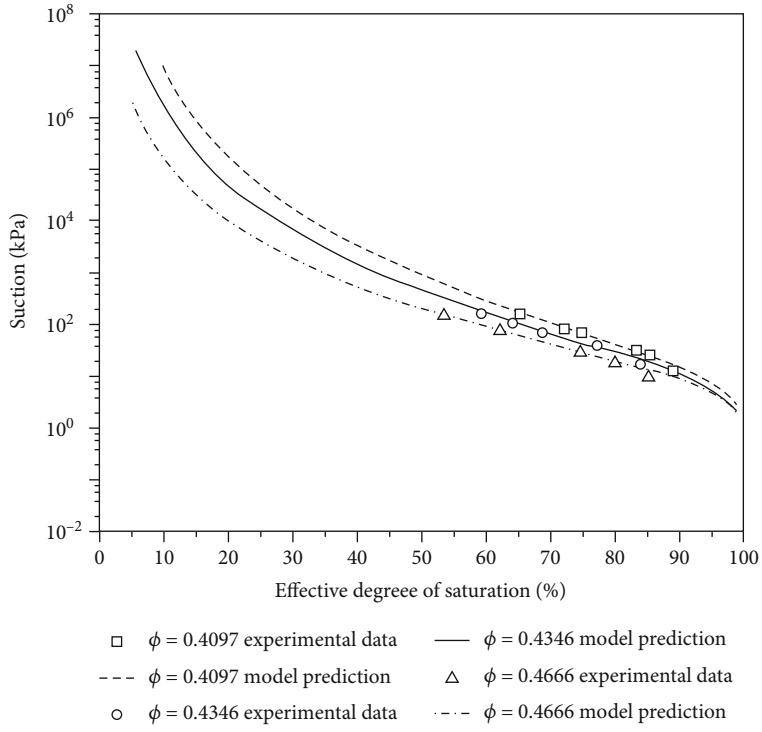

Figure 6: Comparison between experimental and predicted SWRCs with different porosities.

3. Validation

3.1. Sample Preparation and Test Procedure. In order to verify Eq. (17), a pressure-plate system is used to determine SWRCs at different porosities. The setup of the experimental system is shown in Figure 3. A cylindrical soil sample (70 mm in diameter and 20 mm in height) enclosed tightly in a cutting ring is placed on a ceramic disk, and the ceramic disk (with air entry value 500 kPa) connects well with the bottom. With

Table 1: Values of $\{d_1, d_2, d_3, d_4\}$ in Eq. (17) for two different soils.

Parameters	d_1 (kPa)	d_2	d_3	d_4
FEBEX bentonite [24]	4.94×10^5	2.243	26.616	-68.846
Boom clay [28]	0.0176	-11.211	-0.675	10.493

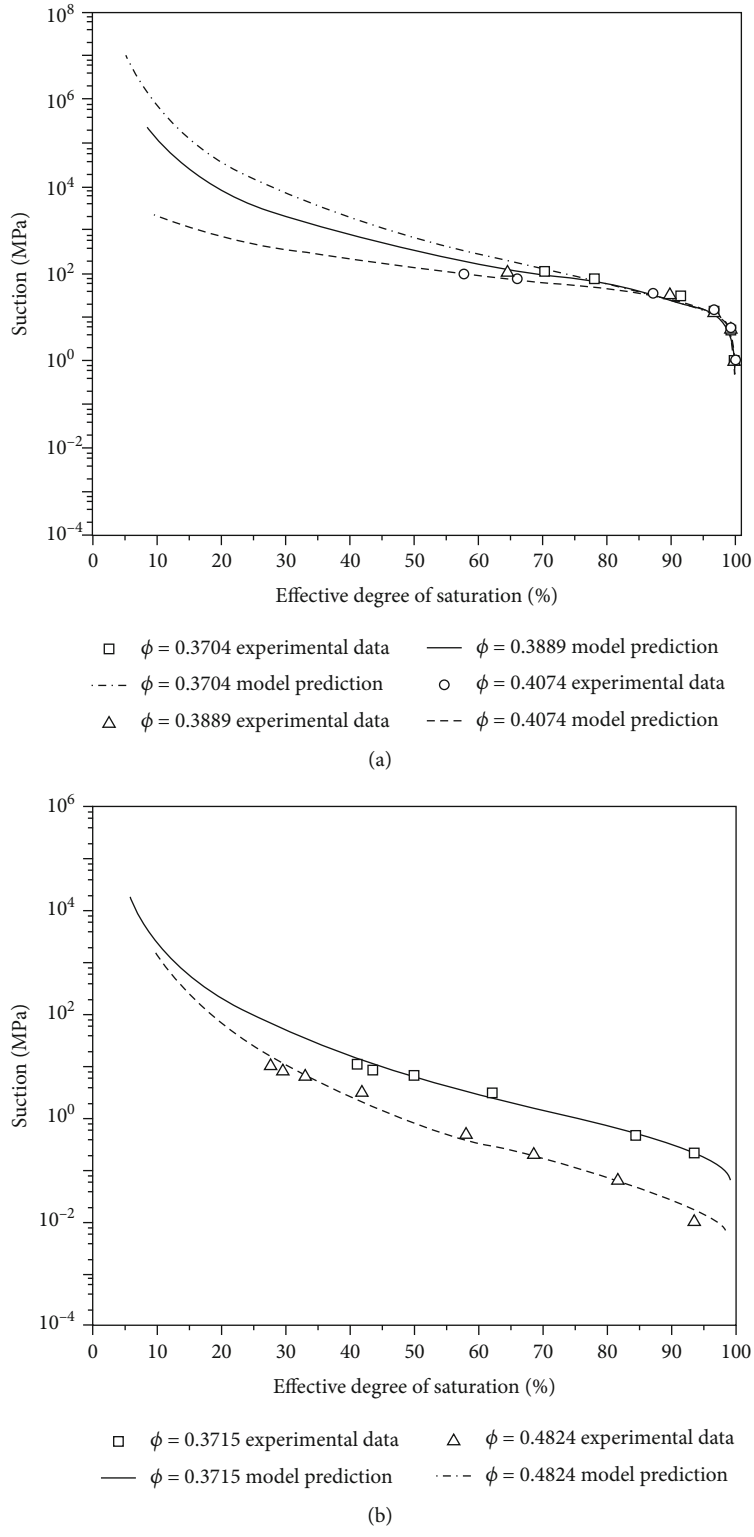

Figure 7: Comparison between model-predicted and literature results: (a) FEBEX bentonite and (b) Boom clay.

the application of air pressure, water flows out from the soil sample to a chamber and the mass of water is measured by a balance.

A kind of loamy sand (83.92% sand, 14.19% silt, and 1.89% clay) extracted from the Three Gorges Region, China, was used as test material. According to the specification of soil test, three samples were prepared and labeled as L1, L2, and L3 (Figure 4), and the corresponding porosities were 0.4666, 0.4346, and 0.4097, respectively. The test started with saturated soil and was carried out in room temperature

(20°C). The degree of saturation corresponding to each suction step was calculated from weighing the water outflow, the soil sample over the test, and the dry sample after drying in an oven.

3.2. Validation against the Experimental Results. The test data for loamy sand with all porosities was adopted to verify Eq. (17). There are four parameters, $\{d_1, d_2, d_3, d_4\}$, in the proposed SWRC model. The parameters are calibrated by using a nonlinear least squares (NLS) fitting method: $d_1 = 0.0115$ kPa, $d_2 = -9.626$, $d_3 = -4.631$, and $d_4 = 20.100$, respectively.

Figure 5 shows the comparison between the model-predicted suctions and the test data for loamy sand. The predicted suctions are in good agreement with the test data, with most discrepancies less than 10%. The measured and predicted SWRCs using the proposed model at different porosities are shown in Figure 6. It can be seen that the predicted SWRCs by the proposed model match well with the experimental data, which indicates that Eq. (17) successfully reproduces the influence of porosity on the SWRC. Figure 6 also shows that both the calculated and measured suctions decrease with the increase of porosity, and the shape and position of SWRCs change obviously with different porosities.

3.3. Validation against Literature Data. In order to further examine the applicability of the proposed model, the experimental data for two different soils found in literature are used.

The first is FEBEX bentonite (clay: 92%; silt and sand: 8%), which is a kind of engineered clay [29]. Three dry densities were chosen here; they are $\rho_{d1} = 1.6\,\text{g/cm}^3$, $\rho_{d2} = 1.65\,\text{g/cm}^3$, and $\rho_{d3} = 1.7\,\text{g/cm}^3$, respectively. The test temperature was 20°C. The porosity was calculated as $\phi = 1 - \rho_d/\rho_s$, where $\rho_s = 2.7\,\text{g/cm}^3$. So, the corresponding porosities of the three samples are $\phi_1 = 0.4074$, $\phi_2 = 0.3889$, and $\phi_3 = 0.3074$, respectively.

The second is Boom clay [33]. This material was obtained by compacting natural Boom clay. The Boom clay (10–20% smectite, 20–30% illite, and 20–30% kaolinite) has a plastic limit of 29%, a liquid limit of 56%, and a specific gravity of 2.7, and half of the particles are smaller than 2 μm. The tested samples were prepared at dry densities of $1.37\,\text{g/cm}^3$ and $1.67\,\text{g/cm}^3$, and the corresponding void ratios are 0.932 and 0.591, respectively. So, the porosities of the two samples are 0.4824 and 0.3715, respectively. The test temperature was kept at 22°C.

The four parameters, $\{d_1, d_2, d_3, d_4\}$, in Eq. (17) are calculated by using the NLS method and listed in Table 1. In Figure 7, the experimental data for the two different soils are fitted with Eq. (17). It reveals very good agreements between the model predictions and experimental data, with negligible discrepancies.

4. Conclusions

A theoretical model is developed to describe the influence of porosity on SWRC. The model is derived for a three-phase mixture with an idealized pore structure. The idealized air bubble shape and pore system meet the equivalence of macroscopic physical effects. On this basis, a SWRC model is proposed, where suction is expressed as a function of porosity and effective saturation. There are four characterization parameters in the model, $\{d_1, d_2, d_3, d_4\}$, with clear physical meaning. d_1 is related to the surface tension; d_2 is related to porosity; d_3 represents the combined effect of temperature, hysteresis effects, and other factors; and d_4 is only related to porosity. An experimental verification of this model was carried out on SWRCs of loamy sand. The model predictions are close to the test results, which also show that suction decreases with the increase of porosity, and the shape and position of SWRCs change obviously with different porosities. The predictions of the proposed model were also compared with the experimental results for FEBEX bentonite and Boom clay in published articles. The good agreements show that the SWRC model is reliable and feasible for wide soils.

Data Availability

The data used to support the findings of this study are included within the article.

Conflicts of Interest

The authors declare that they have no conflicts of interest.

Acknowledgments

This research was supported by the National Key Research and Development Program of China (grant number 2017YFC1501100), the National Nature Science Foundation of China (grant numbers 51939004 and 51279090), and the Open Fund of Key Laboratory of Geological Hazards on Three Gorges Reservoir Area, Ministry of Education, China Three Gorges University (grant number 2020KDZ11).

References

[1] C. A. Burger and C. D. Shackelford, "Soil-water characteristic curves and dual porosity of sand–diatomaceous earth mixtures," *Journal of Geotechnical and Geoenvironmental Engineering*, vol. 127, no. 9, pp. 790–800, 2001.

[2] M. Y. Fattah, N. M. Salim, and E. J. Irshayyid, "Determination of the soil–water characteristic curve of unsaturated bentonite–sand mixtures," *Environmental Earth Sciences*, vol. 76, no. 5, p. 201, 2017.

[3] S. Assouline, "Modeling the relationship between soil bulk density and the water retention curve," *Vadose Zone Journal*, vol. 5, no. 2, pp. 554–563, 2006.

[4] X. Zhang, Y. Wu, E. Zhai, and P. Ye, "Coupling analysis of the heat-water dynamics and frozen depth in a seasonally frozen zone," *Journal of Hydrology*, p. 125603, 2020.

[5] A. Zhou, Y. Fan, W. Cheng, and J. Zhang, "A fractal model to interpret porosity-dependent hydraulic properties for unsaturated soils," *Advance in Civil Engineering*, vol. 2019, article 3965803, pp. 1–13, 2019.

[6] M. Aubertin, M. Mbonimpa, B. Bussière, and R. P. Chapuis, "A model to predict the water retention curve from basic

geotechnical properties," *Canadian Geotechnical Journal*, vol. 40, no. 6, pp. 1104–1122, 2003.

[7] R. H. Brooks and A. T. Corey, 1964, Hydraulic properties of porous media. Hydrology paper no. 3, Colorado State University, Fort Collins, CO.

[8] D. G. Fredlund and A. Xing, "Equations for the soil-water characteristic curve," *Canadian Geotechnical Journal*, vol. 31, no. 4, pp. 521–532, 1994.

[9] X. S. Li, "Modelling of hysteresis response for arbitrary wetting/drying paths," *Computers and Geotechnics*, vol. 32, no. 2, pp. 133–137, 2005.

[10] Y. Mualem, "A new model for predicting the hydraulic conductivity of unsaturated porous media," *Water Resources Research*, vol. 12, pp. 564–566, 1976.

[11] M. T. van Genuchten, "A closed-form equation for predicting the hydraulic conductivity of unsaturated soils," *Soil Science Society of America Journal*, vol. 44, no. 5, pp. 892–898, 1980.

[12] Q. Meng, H. Wang, M. Cai, W. Xu, X. Zhuang, and T. Rabczuk, "Three-dimensional mesoscale computational modeling of soil-rock mixtures with concave particles," *Engineering Geology*, vol. 277, article 105802, 2020.

[13] Q. Meng, H. Wang, M. He, J. Gu, and L. Yang, "Displacement prediction of water-induced landslides using a recurrent deep learning model," *European Journal of Environmental and Civil Engineering*, vol. 2020, pp. 1–15, 2020.

[14] L. Yan, W. Xu, H. Wang et al., "Drainage controls on the Donglingxing landslide (China) induced by rainfall and fluctuation in reservoir water levels," *Landslides*, vol. 16, no. 8, pp. 1583–1593, 2019.

[15] C. Zhu, Z. Yan, Y. Lin, F. Xiong, and Z. Tao, "Design and application of a monitoring system for a deep railway foundation pit project," *IEEE Access*, vol. 7, pp. 107591–107601, 2019.

[16] C. Zhu, X. Xu, and W. Liu, "Softening damage analysis of gypsum rock with water immersion time based on laboratory experiment," *IEEE Access*, vol. 7, pp. 125575–125585, 2019.

[17] C. Zhu, M. He, M. Karakus, X. Cui, and Z. Tao, "Investigating toppling failure mechanism of anti-dip layered slope due to excavation by physical modelling," *Rock Mechanics and Rock Engineering*, vol. 53, no. 11, pp. 5029–5050, 2020.

[18] D. Mašín, "Predicting the dependency of a degree of saturation on void ratio and suction using effective stress principle for unsaturated soils," *International Journal for Numerical and Analytical Methods in Geomechanics*, vol. 34, no. 1, pp. 73–90, 2010.

[19] D. Sheng and A. Zhou, "Coupling hydraulic with mechanical models for unsaturated soils," *Canadian Geotechnical Journal*, vol. 48, no. 5, pp. 826–840, 2011.

[20] D. A. Sun, D. C. Sheng, H. B. Cui, and S. W. Sloan, "A density-dependent elastoplastic hydro-mechanical model for unsaturated compacted soils," *International Journal for Numerical and Analytical Methods in Geomechanics*, vol. 31, no. 11, pp. 1257–1279, 2007.

[21] A. Tarantino, "A water retention model for deformable soils," *Geotechnique*, vol. 59, no. 9, pp. 751–762, 2009.

[22] S. J. Wheeler, R. S. Sharma, and M. S. R. Buisson, "Coupling of hydraulic hysteresis and stress-strain behaviour in unsaturated soils," *Geotechnique*, vol. 53, no. 1, pp. 41–54, 2003.

[23] S. C. Florian and R. Horn, "Modeling the soil water retention curve for conditions of variable porosity," *Vadose Zone Journal*, vol. 4, pp. 602–613, 2005.

[24] D. Gallipoli, "A hysteretic soil-water retention model accounting for cyclic variations of suction and void ratio," *Géotechnique*, vol. 62, no. 7, pp. 605–616, 2012.

[25] D. Gallipoli, S. J. Wheeler, and M. Karstunen, "Modelling the variation of degree of saturation in a deformable unsaturated soil," *Géotechnique*, vol. 53, no. 1, pp. 105–112, 2003.

[26] S. Huang, S. L. Barbour, and D. G. Fredlund, "Development and verification of a coefficient of permeability function for a deformable unsaturated soil," *Canadian Geotechnical Journal*, vol. 35, no. 3, pp. 411–425, 1998.

[27] M. Nuth and L. Laloui, "Advances in modelling hysteretic water retention curve in deformable soils," *Computers and Geotechnics*, vol. 35, no. 6, pp. 835–844, 2008.

[28] A. Zhou, D. Sheng, and J. P. Carter, "Modelling the effect of initial density on soil-water characteristic curves," *Géotechnique*, vol. 62, no. 8, pp. 669–680, 2012.

[29] F. Tong, L. Jing, and T. Bin, "A water retention curve model for the simulation of coupled thermo-hydro-mechanical processes in geological porous media," *Transport in Porous Media*, vol. 91, no. 2, pp. 509–530, 2012.

[30] L. A. Richards, "Capillary conduction of liquids through porous mediums," *Journal of Applied Physics*, vol. 1, no. 5, pp. 318–333, 1931.

[31] C. Liu, F. Tong, L. Biao, and Z. Yitong, "A water retention curve model describing the effect of temperature," *European Journal of Soil Science*, vol. 71, pp. 44–54, 2020.

[32] X. Zhang, C. Zhao, Y. Liu, and G. Cai, "Modeling study of the relationship between deformation and water retention curve," *China Civil Engineering Journal*, vol. 44, pp. 119–126, 2011.

[33] E. Romero, A. Gens, and A. Lloret, "Suction effects on a compacted clay under non-isothermal conditions," *Géotechnique*, vol. 53, no. 1, pp. 65–81, 2003.